

Facile Synthesis and Study of Microporous CANAL-Tröger's Base Ladder Polymers for Membrane Air Separation

Xiaohua Ma,^a Holden W. H. Lai,^b Yingge Wang,^a Abdulrahman Alhazmi,^a
Yan Xia,^{b*} Ingo Pinnau^{a*}

^a Functional Polymer Membranes Group, Advanced Membranes and Porous Materials Center, Division of Physical Science and Engineering, Chemical Engineering Program, King Abdullah University of Science and Technology (KAUST), Thuwal 23955-6900, KSA.

^b Department of Chemistry, Stanford University, Stanford, California 94305, United States.

Corresponding authors:

^{a*} E-mail: ingo.pinnau@kaust.edu.sa;

^{b*} E-mail: yanx@stanford.edu

Keywords: ladder polymer, microporosity, Tröger's base, gas separation membranes

Abstract

We report the facile synthesis and study of two soluble microporous ladder polymers, CANAL-TBs, by combining catalytic norbornene-arene annulation (CANAL) and Tröger's Base (TB) formation. The polymers were synthesized in two steps from commercially available chemicals in high yields. CANAL-TBs easily formed mechanically robust films. CANAL-TBs were thermally stable up to 440 °C and exhibited very high Brunauer-Teller-Emmett surface areas of 900-1000 m² g⁻¹. The gas separation performance of the CANAL-TBs for the O₂/N₂ pair is located between the 2008 and 2015 permeability/selectivity upper bounds. After 300 days of aging, CANAL-TBs still exhibited O₂ permeability of 200-500 barrer with O₂/N₂ selectivity of about 5. The polymer with more methyl substituents exhibited higher permeability and slightly larger intersegmental spacing as revealed by WAXS, presumably due to more frustrated chain packing. The facile synthesis, excellent mechanical properties, and promising air separation performance of the CANAL-TB polymers make them attractive membrane materials for various air separation applications, such as aircraft on-board nitrogen generation and oxygen enrichment for combustion.

Solution-processible ladder polymers of intrinsic microporosity (PIMs) are an emerging class of membrane gas separation materials.¹⁻⁷ Rigid and contorted ladder motifs in the polymer backbone are key to induce frustrated polymer chain packing, leading to high fractional free volume and microporosity in polymers. The gas separation properties of PIMs depend strongly on the molecular structures and micropore size distributions.⁸⁻¹¹ To develop highly permeable *and* selective polymer membranes, it is essential to have both ultramicropores ($< 7 \text{ \AA}$) for highly selective gas transport and larger interconnected micropores ($> 10 \text{ \AA}$) for fast gas permeation. This general concept resulted in systematic development of various PIMs with very high permeability and generally moderate selectivity for several important gas pairs,^{8, 12-18} including O_2/N_2 , H_2/N_2 , H_2/CH_4 and, more recently, pure-gas CO_2/N_2 and CO_2/CH_4 , redefining upper bounds in the separation performance.¹⁹⁻²⁰

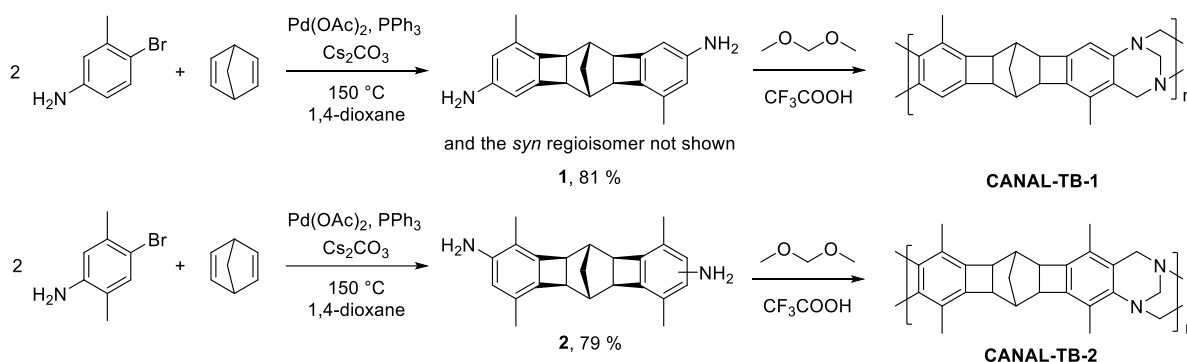
PIMs were first developed based on polycondensation of tetrafluoroterephthalonitrile with contorted bisphenol motifs based on most commonly spirobisindane (SBI), spirobifluorene (SBF), and triptycene.^{8, 13, 21-22} In 2013, the McKeown group reported using Tröger's base (TB) formation as a method to synthesize ladder PIMs (TB-PIMs) via reaction of ladder or spirocyclic aryl diamines with dimethoxymethane in acid.^{14-15, 23-25} The TB linkage consists of a rigid, bent, and chiral methanodibenzodiazocine structure. TB motifs have also been used as building blocks to synthesize pseudo-ladder PIM polyimides (PIM-PIs), which displayed excellent gas separation performance.²⁶⁻³¹ The bisphenol condensation and TB formation have been the dominating methods for the synthesis of microporous ladder polymers. The Xia group recently reported an efficient catalytic arene-norbornene annulation (CANAL) polymerization to synthesize rigid hydrocarbon ladder polymers using aryl bromides and norbornadiene as the monomers.³²⁻³⁶ CANAL polymerization yields rigid and contorted norbornyl benzocyclobutene ladder backbones that result in high surface areas and microporosity. The CANAL ladder polymers from simple dibromobenzenes and norbornadiene give ribbon-like rigid chain conformations. CANAL polymer films exhibited high gas permeability but low selectivity.³⁶ Interestingly, even simple short aliphatic substituents were found to significantly affect the permeability without affecting the selectivity.³⁶ We became interested in modifying the backbone of CANAL polymers and investigating its effect on gas separation performance.

We now report a series of ladder polymers, CANAL-TBs, fusing CANAL and TB motifs. Their synthesis was facile and high-yielding, requiring only two steps from commercially available starting materials. These CANAL-TB polymers easily formed films with excellent mechanical properties, and exhibited significantly improved O_2/N_2 selectivity to ~ 5 without reduction in O_2 permeability compared to the recently reported pure CANAL hydrocarbon

polymers.³⁶ The facile synthesis, robust mechanical properties, and excellent air separation performance make the CANAL-TB polymers promising membrane materials for air separation applications.

We chose two commercially available *p*-bromoanilines and norbornadiene to synthesize two norbornyl bis(aminobenzocyclobutene) ladder aryl diamines, **1** and **2**, with two and four methyl substituents, respectively (Scheme 1). CANAL reaction using 2 mol% Pd(OAc)₂, 4 mol% PPh₃, and 1 eq. Cs₂CO₃ in 1,4-dioxane at 150 °C proceeded smoothly to give **1** and **2** in 80% yield. The *ortho*-methyl group on bromoanilines was important to achieve high yield and selectivity in CANAL. Because of the exclusive *exo*-selectivity of CANAL, these CANAL diamines exhibited a “W” shape (existing in *syn* and *anti*-diamine isomers). The diamines **1** and **2** were then polymerized via TB formation^{14, 23} by reacting with dimethoxymethane in neat CF₃COOH to produce CANAL-TB-1 and CANAL-TB-2, respectively. The resulting polymers were soluble in dichloromethane and chloroform.

Scheme 1. Synthetic Routes of the CANAL-TB Ladder Polymers.

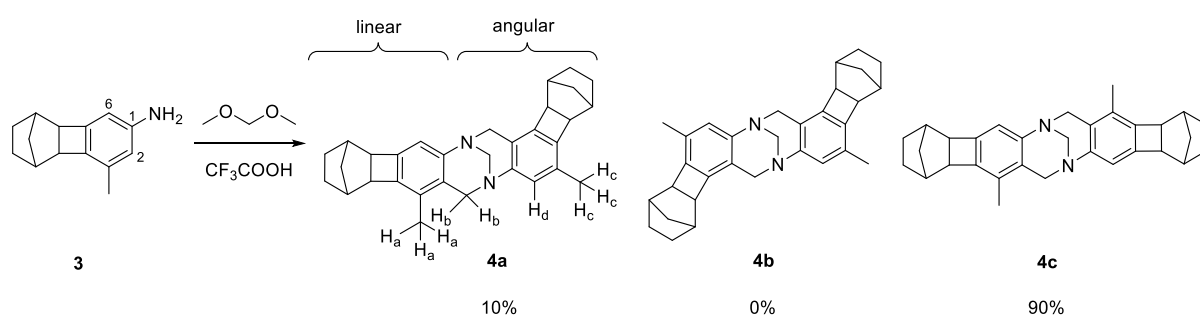


¹H NMR spectroscopy of the isolated polymers showed complete preservation of all the expected signals from the CANAL motif (Figure S1), especially the characteristic signal from benzocyclobutene around 3.1 ppm, suggesting its stability under the strongly acidic conditions for TB formation. New signals around 3.7–4.8 ppm corresponding to the TB linkages also appeared. For CANAL-TB-1, no aromatic proton signals were observed as expected, whereas for CANAL-TB-2, one peak at 6.7 ppm was observed. Integrations of all these peaks yielded ratios consistent with those expected for the proposed TB ladder backbone. FT-IR spectroscopy of the polymers showed the disappearance of N-H stretch peaks at 3000–3500 cm⁻¹, which were strong in the CANAL diamines (Figure S2).

Because CANAL-TB-1 has two possible aromatic sites for TB formation, we carried out a TB model reaction using singly fused ladder compound **3** to probe the regioselectivity in TB

formation for CANAL-TB-1 (Scheme 2). The regiochemistry of the products was determined by 1-D ^1H nuclear Overhauser effect (NOE) experiments, by saturating the methyl frequencies. For the linear fusion, where the TB formation occurs at the 2 position, NOE correlation is expected between the benzylic protons H_a and the methylene protons H_b in TB; whereas in the angular fusion, where the TB formation occurs at the 6 position, NOE correlation is expected between the benzylic protons H_c and the aromatic proton H_d (Scheme 2). Using this NOE method, of the three potential regioisomers **4a-c**, we only identified **4a** and **4c** at a 1:9 ratio (Figure S3-7). Because **4a** contains one linear and one angular fusion and both fusions in **4c** are linear, the result of this model reaction suggests that the ratio of angular vs linear fusion in the backbone of CANAL-TB-1 may be $\sim 1:19$. Therefore, CANAL-TB-1 and CANAL-TB-2 may be expected to have similarly extended backbone conformations.

Scheme 2. Model Reaction to Assess the Regio-Selectivity of the TB Formation.



In this study, isotropic films with thicknesses of ~ 40 μm were easily obtained by casting from CANAL-TBs' chloroform solutions. The films exhibited excellent mechanical properties, still maintaining their structural integrity after repeated sharp bending and twisting (Figure 1). We measured the ultimate tensile strength of CANAL-TB-1 and CANAL-TB-2 to be 63 and 46 MPa, respectively, similar to that of widely investigated PIMs—PIM-1 (30–50 MPa)³⁷⁻³⁹ and PIM-TRIP-TB (45 MPa).¹⁵ The films were also remarkably flexible with high elongation at break of 15 and 28% for CANAL-TB-1 and CANAL-TB-2, respectively (Figure S8, Table S1). The Young's modulus was determined to be 1.6 and 0.42 GPa for CANAL-TB-1 and CANAL-TB-2, respectively, which is comparable to the stiffness of PIM-1 and PIM-TRIP-TB (Table S1).

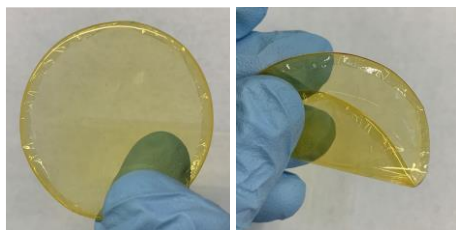


Figure 1. Photos of CANAL-TB films demonstrating its mechanical flexibility.

Both CANAL-TB polymers exhibited very high thermal stability with the onset of thermal decomposition at 5% mass loss ($T_{d,5\%}$) around 440 °C (Figure S9), and high carbonization yields of 74 and 69% for CANAL-TB-1 and CANAL-TB-2, respectively, at 800 °C.

We investigated the BET surface areas and microporosity of the CANAL-TB polymers by N_2 sorption at 77 K up to 1 bar. Both polymers exhibited Type II sorption isotherms and abundant microporosity with large nitrogen uptake at low pressure ($p/p_0 < 0.05$) (Figure 2a). CANAL-TB-1 and CANAL-TB-2 showed high BET surface areas of 881 and 987 $m^2 g^{-1}$, respectively (Table 1), which are comparable to the highest reported surface areas from soluble PIMs, such as PIM-Trip-TB (899 $m^2 g^{-1}$),¹⁵ PIM-BTrip-TB (870 $m^2 g^{-1}$),²⁴ PIM-EA-TB (1028 $m^2 g^{-1}$),²³ PIM-TMN-Trip (1050 $m^2 g^{-1}$),¹⁶ and PIM-TMN-SBI (1015 $m^2 g^{-1}$).¹⁶ The higher BET surface area for CANAL-TB-2 compared to that of CANAL-TB-1 may be attributed to the more frustrated chain packing imposed by two additional methyl substituents. We derived the pore size distributions from N_2 sorption isotherms by non-local density functional theory (NLDFT) using the standard slit carbon model (Figure 2b).⁴⁰ Both polymers exhibited abundant micropores with pore width in the range of ~11 to 15 Å and ultramicropores <7 Å. The ultramicropore distributions appeared very similar between the two polymers, despite their different gas permeation properties as discussed below. The difference in gas permeation between the two polymers may result from structural differences in pore size (<5 Å) that are too small for N_2 to access at 77 K in the N_2 sorption measurement.

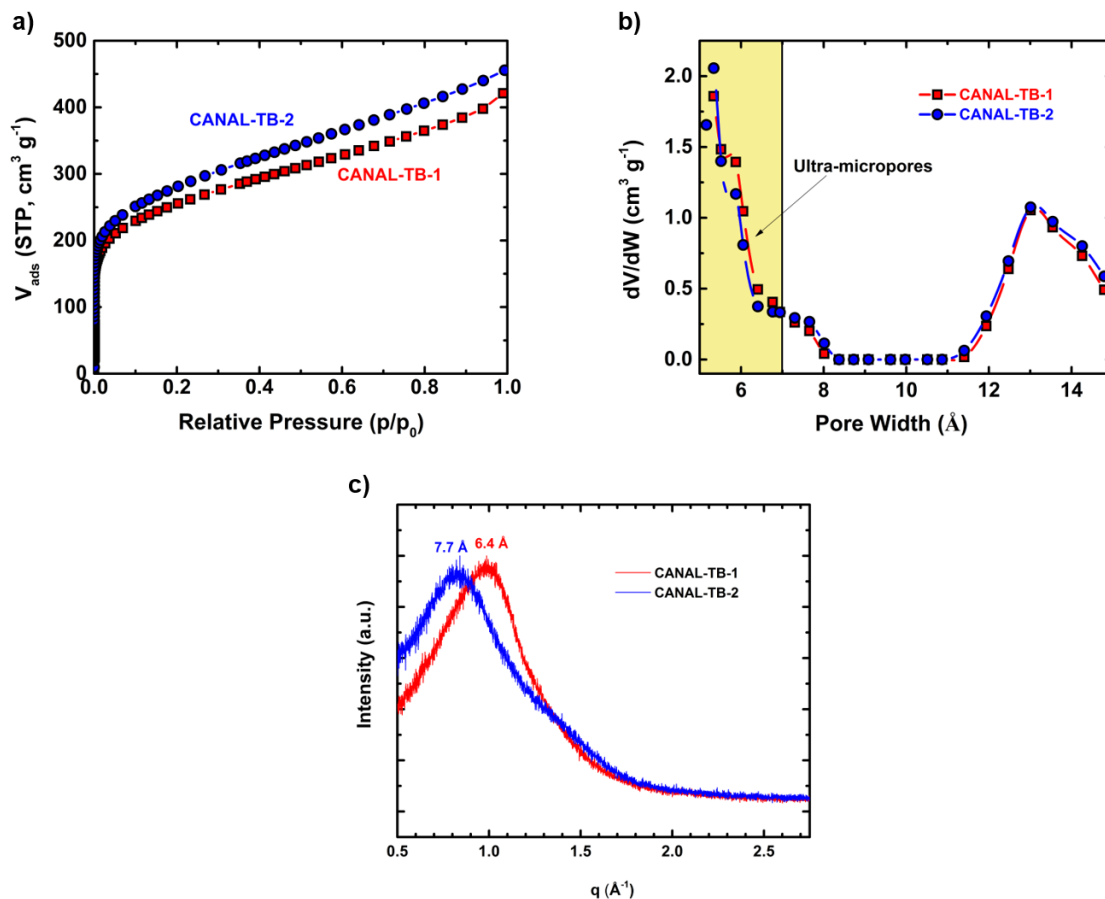


Figure 2. Characterization of microporosity of CANAL-TB polymers. a) N₂ sorption isotherms of CANAL-TB-1 and CANAL-TB-2 at 77 K; b) pore size distribution of CANAL-TB-1 and CANAL-TB-2 derived from N₂ adsorption isotherms by non-local density functional theory using the standard slit carbon model;⁴⁰ c) wide-angle X-ray scattering of CANAL-TB-1 and CANAL-TB-2 films. Both films were soaked in methanol and then dried in a vacuum oven at 120 °C for 24 h.

Wide-angle X-ray scattering of the two polymer films indicated their amorphous structures and revealed the difference in their intersegmental spacing (Figure 2c). CANAL-TB-1 displayed a broad peak with maximum intensity at $q = 1.0 \text{ \AA}^{-1}$, corresponding to 6.4 \AA . CANAL-TB-2 displayed a broad peak shifted toward lower q with a larger d -spacing of 7.7 \AA , indicating its larger intersegmental spacing, which again may be attributed to its additional methyl substituents.

We next evaluated the gas permeation properties of CANAL-TB-1 and CANAL-TB-2 films for H₂, N₂, O₂, CH₄, and CO₂ at 2 bar upstream pressure and 35°C using the constant volume/variable pressure method (Table 1). Previously reported TB-containing ladder PIMs, PIM-TRIP-TB, PIM-EA-TB, and PIM-MP-TB, are included in Table 1 for comparison.

Table 1. Gas Permeability and Gas-Pair Selectivity of CANAL-TB-1 and CANAL-TB-2 (T = 35 °C; p = 2 bar) and Related Tröger’s Base-Containing PIMs.

Polymer (thickness in μm)	Permeability (barrer)					Ideal selectivity (-)			
	H ₂	N ₂	O ₂	CH ₄	CO ₂	H ₂ /N ₂	H ₂ /CH ₄	O ₂ /N ₂	CO ₂ /CH ₄
CANAL-TB-1 ^a	2760	97	463	121	1678	28.5	22.8	4.8	13.9
Aged 300 d (39 μm)	1163	39	204	53	749	29.8	22.0	5.2	14.1
CANAL-TB-2 ^a	3608	162	747	205	2520	22.3	17.6	4.6	12.3
Aged 300 d (39 μm)	2452	110	528	129	1751	22.4	19.1	4.8	13.6
PIM-TRIP-TB ^{b, c}	8039	629	2718	905	9709	12.8	8.9	4.3	10.7
Aged 100 d (132 μm)	4740	189	1073	218	3951	25.0	21.7	5.7	18.1
PIM-EA-TB (181 μm) ^{b, d}	7760	525	2150	699	7140	14.8	11.1	4.1	10.2
PIM-MP-TB (94 μm) ^{b, e}	4050	200	999	264	3500	20.3	15.3	5.0	13.3

^a Soaked in methanol and then dried at 120 °C under vacuum for 24 h. ^b Soaked in methanol and then air dried; tested at T = 25 °C; p = 1 bar. ^c ref. 15; ^d ref. 14; ^e ref. 25.

The order of gas permeabilities for both CANAL-TB-1 and CANAL-TB-2 was $\text{PH}_2 > \text{PCO}_2 > \text{PO}_2 > \text{PCH}_4 > \text{PN}_2$, which is consistent with those of other reported TB-containing PIM films, such as PIM-EA-TB,¹⁴ PIM-MP-TB,²⁵ and aged PIM-Trip-TB.¹⁵ Freshly prepared CANAL-TB-1 and CANAL-TB-2 films exhibited O₂ permeability of 463 and 747 barrer and an O₂/N₂ selectivity of 4.8 and 4.6, respectively. Highly microporous PIM films commonly experience physical aging with significantly reduced gas permeability over time and often an increase in selectivity.^{6, 11} Therefore, we studied the gas permeation for CANAL-TB-1 and CANAL-TB-2 films that were aged at room temperature. After 300 days of physical aging, both films still showed promising performance for air separation applications with O₂ permeability of 204 and 528 barrer for CANAL-TB-1 and CANAL-TB-2, respectively. Interestingly, the percentage decrease in O₂ permeability was smaller for the more permeable CANAL-TB-2 (29% decrease from the freshly prepared film) than for CANAL-TB-1 (56% decrease from the freshly prepared film). Aging also resulted in moderate increases in selectivity for all gas pairs listed in Table 1. This behavior is different from what was previously observed in the aging of other PIMs, which showed significant boosts in selectivity and significant reduction in permeability, as shown for PIM-TRIP-TB (Table 1).^{6, 11, 41} We hypothesize that the reduction in gas permeability upon aging without significant increase in selectivity for CANAL-TB films may be due to the

collapse of larger micropores ($>10 \text{ \AA}$) without generation of size-selective ultramicropores ($<7 \text{ \AA}$). Nevertheless, the performance after long-term aging (Table 1), O_2/N_2 selectivity of 5.2 and 4.8 for CANAL-TB-1 and CANAL-TB-2, respectively, remained attractive for air separation application, including membrane production of oxygen-enriched air for combustion and nitrogen generation from air for fuel tank inerting on aircrafts, where materials with high O_2 permeability and moderate O_2/N_2 selectivity are desirable to provide compact and lightweight systems.^{3, 42}

To investigate details of physical aging, we determined diffusion coefficients for fresh and 300-day old samples using the time-lag method.⁴³ Table S2 shows the diffusion coefficients for N_2 , O_2 , CH_4 , and CO_2 as well as the diffusion selectivity and solubility selectivity for O_2/N_2 and CO_2/CH_4 in CANAL-TB films on day 1 and after 300 days. Clearly, aged samples showed significant drop in diffusion coefficients, accompanied by only marginal increase in diffusion selectivity (α_D) for O_2/N_2 and CO_2/CH_4 . On the other hand, physical aging had essentially no effect on O_2/N_2 solubility selectivity, which remained around 1.1.

The O_2/N_2 gas separation performance of CANAL-TB-1 and CANAL-TB-2 is compared to the seminal PIM-1, several other TB-based PIMs, and three commercial membranes used for air separations—Matrimid, polysulfone (PSF), and poly(phenylene oxide) (PPO) (Figure 3). All current commercial membranes have very low permeability and fall below the 1991 upper bound for O_2/N_2 separation.⁴⁴ Since the advent of PIMs, significantly more permeable membrane polymers have been reported, moving up the tradeoff curves to the 2008 and 2015 records.^{19, 45} Like other TB-containing PIMs, the performance of CANAL-TB-1 and CANAL-TB-2 is located between the 2008 and 2015 upper bounds for O_2/N_2 separation, but CANAL-TBs exhibit higher selectivity and lower permeability compared to several other TB-containing PIMs (Figure 3). Notably, the O_2 permeability of CANAL-TBs is still very high. Their performance makes them desired membrane materials for air separation applications that require high O_2 permeability (> 500 barrer) and only moderate O_2/N_2 selectivity (~ 4 -5), such as combustion and fuel tank inerting applications. Their simple two-step high-yielding synthesis from commercial chemicals and excellent mechanical properties of the films are two additional important features that make CANAL-TBs promising membrane polymers for air separations.

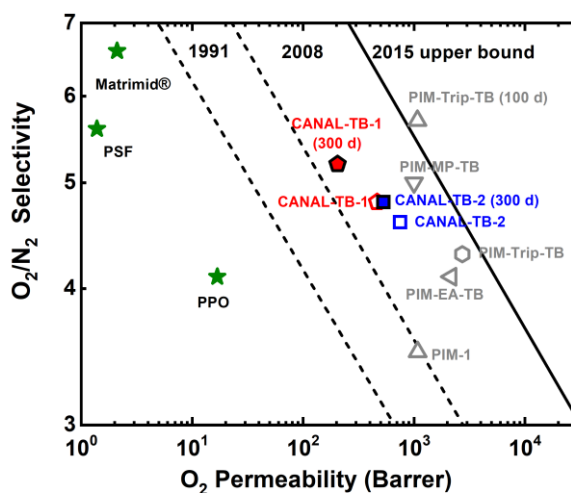


Figure 3. O_2/N_2 separation performance of CANAL-TB-1 and CANAL-TB-2 (open symbols: freshly prepared; closed symbols: aged for 300 days) and previously reported ladder-type PIMs relative to 1991⁴⁴ (dashed line), 2008⁴⁵ (dashed line), and 2015¹⁹ (solid line) upper bounds.

In summary, we report two microporous ladder polymers, CANAL-TB-1 and CANAL-TB-2, with backbones consisting of two rigid ladder motifs, fused norbornyl benzocyclobutene and Tröger's base. Their synthesis from commercially available bromoanilines and norbornadiene was simple and high yielding. CANAL-TBs exhibited excellent thermal stability, robust mechanical properties, and high gas permeability. CANAL-TB-2 with more methyl substituents exhibited a more open internal structure than CANAL-TB-1, as suggested by its larger average intersegmental spacing and higher gas permeability. Films of these polymers showed promising air separation performance. After 300 days of aging, CANAL-TB-1 and CANAL-TB-2 still displayed high O_2 permeability and moderate O_2/N_2 selectivity. The encouraging separation performance, facile synthesis, thermal and chemical stability, and remarkable mechanical properties collectively make these polymers excellent candidates to be further developed into thin-film composite membranes for air separation applications.

ASSOCIATED CONTENT

Supporting Information

Experimental details, NMR and FT-IR spectra, analysis of model reaction, mechanical properties, gas diffusion coefficients, permeability/selectivity trade-offs, 3D MD simulations and FFV of CANAL-TBs. The Supporting Information is available free of charge on the ACS Publications website.

AUTHOR INFORMATION

Corresponding Author

*E-mails: ingo.pinnau@kaust.edu.sa; yanx@stanford.edu

ORCID

Xiaohua Ma: 0000-0002-1667-6342

Holden W. H. Lai: 0000-0002-0090-9594

Yan Xia: 0000-0002-5298-748X

Ingo Pinnau: 0000-0003-3040-9088

Notes

A patent application has been filed for the reported polymers and their applications in membrane gas separation.

ACKNOWLEDGEMENTS

This work was supported by funding (BAS/1/1323-01-01) from King Abdullah University of Science and Technology and the Stanford Natural Gas Initiative. H. W. H. Lai is supported by NSF-GRFP (DGE- 156518).

REFERENCES

1. McKeown, N. B.; Budd, P. M. Polymers of Intrinsic Microporosity (PIMs): Organic Materials for Membrane Separations, Heterogeneous Catalysis and Hydrogen Storage. *Chem. Soc. Rev.* **2006**, *35*, 675-683.
2. Sanders, D. F.; Smith, Z. P.; Guo, R.; Robeson, L. M.; McGrath, J. E.; Paul, D. R.; Freeman, B. D. Energy-Efficient Polymeric Gas Separation Membranes for a Sustainable Future: A Review. *Polymer* **2013**, *54*, 4729-4761.
3. Baker, R. W.; Low, B. T. Gas Separation Membrane Materials: A Perspective. *Macromolecules* **2014**, *47*, 6999-7013.
4. Koros, W. J.; Zhang, C. Materials for Next-Generation Molecularly Selective Synthetic Membranes. *Nat. Mater.* **2017**, *16*, 289.
5. Wang, Y.; Ma, X.; Ghanem, B. S.; Alghunaimi, F.; Pinnau, I.; Han, Y. Polymers of Intrinsic Microporosity for Energy-Intensive Membrane-Based Gas Separations. *Mater. Today Nano* **2018**, *3*, 69-95.
6. Low, Z.-X.; Budd, P. M.; McKeown, N. B.; Patterson, D. A. Gas Permeation Properties, Physical Aging, and Its Mitigation in High Free Volume Glassy Polymers. *Chem. Rev.* **2018**, *118*, 5871-5911.
7. Corrado, T.; Guo, R. Macromolecular Design Strategies Toward Tailoring Free Volume in Glassy Polymers for High Performance Gas Separation Membranes. *Mol. Syst. Des. Eng.* **2020**.

8. Ghanem, B. S.; Swaidan, R.; Ma, X.; Litwiller, E.; Pinnau, I. Energy-Efficient Hydrogen Separation by AB-Type Ladder-Polymer Molecular Sieves. *Adv. Mater.* **2014**, *26*, 6696-6700.
9. Guiver, M. D.; Lee, Y. M. Polymer Rigidity Improves Microporous Membranes. *Science* **2013**, *339*, 284-285.
10. Kim, S.; Lee, Y. M. Rigid and Microporous Polymers for Gas Separation Membranes. *Prog. Polym. Sci.* **2015**, *43*, 1-32.
11. Swaidan, R.; Ghanem, B.; Litwiller, E.; Pinnau, I. Physical Aging, Plasticization and Their Effects on Gas Permeation in "Rigid" Polymers of Intrinsic Microporosity. *Macromolecules* **2015**, *48*, 6553-6561.
12. Budd, P. M.; Msayib, K. J.; Tattershall, C. E.; Ghanem, B. S.; Reynolds, K. J.; McKeown, N. B.; Fritsch, D. Gas Separation Membranes from Polymers of Intrinsic Microporosity. *J. Membr. Sci.* **2005**, *251*, 263-269.
13. Bezzu, C. G.; Carta, M.; Tonkins, A.; Jansen, J. C.; Bernardo, P.; Bazzarelli, F.; McKeown, N. B. A Spirobifluorene-Based Polymer of Intrinsic Microporosity with Improved Performance for Gas Separation. *Adv. Mater.* **2012**, *24*, 5930-5933.
14. Carta, M.; Malpass-Evans, R.; Croad, M.; Rogan, Y.; Jansen, J. C.; Bernardo, P.; Bazzarelli, F.; McKeown, N. B. An Efficient Polymer Molecular Sieve for Membrane Gas Separations. *Science* **2013**, *339*, 303-307.
15. Carta, M.; Croad, M.; Malpass-Evans, R.; Jansen, J. C.; Bernardo, P.; Clarizia, G.; Friess, K.; Lanč, M.; McKeown, N. B. Triptycene Induced Enhancement of Membrane Gas Selectivity for Microporous Tröger's Base Polymers. *Adv. Mater.* **2014**, *26*, 3526-3531.
16. Rose, I.; Bezzu, C. G.; Carta, M.; Comesaña-Gándara, B.; Lasseguette, E.; Ferrari, M. C.; Bernardo, P.; Clarizia, G.; Fuoco, A.; Jansen, J. C.; Hart, Kyle E.; Liyana-Arachchi, T. P.; Colina, C. M.; McKeown, N. B. Polymer Ultrapermability from the Inefficient Packing of 2D Chains. *Nat. Mater.* **2017**, *16*, 932.
17. Luo, S.; Zhang, Q.; Zhu, L.; Lin, H.; Kazanowska, B. A.; Doherty, C. M.; Hill, A. J.; Gao, P.; Guo, R. Highly Selective and Permeable Microporous Polymer Membranes for Hydrogen Purification and CO₂ Removal from Natural Gas. *Chem. Mater.* **2018**, *30*, 5322-5332.
18. He, Y.; Benedetti, F. M.; Lin, S.; Liu, C.; Zhao, Y.; Ye, H.-Z.; Van Voorhis, T.; De Angelis, M. G.; Swager, T. M.; Smith, Z. P. Polymers with Side Chain Porosity for Ultrapermable and Plasticization Resistant Materials for Gas Separations. *Adv. Mater.* **2019**, *31*, 1807871.
19. Swaidan, R.; Ghanem, B.; Pinnau, I. Fine-Tuned Intrinsically Ultramicroporous Polymers Redefine the Permeability/Selectivity Upper Bounds of Membrane-Based Air and Hydrogen Separations. *ACS Macro Lett.* **2015**, *4*, 947-951.
20. Comesaña-Gándara, B.; Chen, J.; Bezzu, C. G.; Carta, M.; Rose, I.; Ferrari, M.-C.; Esposito, E.; Fuoco, A.; Jansen, J. C.; McKeown, N. B. Redefining the Robeson Upper Bounds for CO₂/CH₄ and CO₂/N₂ Separations Using a Series of Ultrapermable Benzotriptycene-Based Polymers of Intrinsic Microporosity. *Energy Environ. Sci.* **2019**, *12*, 2733-2740.
21. Budd, P. M.; Elabas, E. S.; Ghanem, B. S.; Makhseed, S.; McKeown, N. B.; Msayib, K. J.; Tattershall, C. E.; Wang, D. Solution-Processed, Organophilic Membrane Derived from a Polymer of Intrinsic Microporosity. *Adv. Mater.* **2004**, *16*, 456-459.
22. Budd, P. M.; Ghanem, B. S.; Makhseed, S.; McKeown, N. B.; Msayib, K. J.; Tattershall, C. E. Polymers of Intrinsic Microporosity (PIMs): Robust, Solution-Processable, Organic Nanoporous Materials. *Chem. Commun.* **2004**, 230-231.
23. Carta, M.; Malpass-Evans, R.; Croad, M.; Rogan, Y.; Lee, M.; Rose, I.; McKeown, N. B. The Synthesis of Microporous Polymers Using Tröger's Base Formation. *Polym. Chem.* **2014**, *5*, 5267-5272.
24. Rose, I.; Carta, M.; Malpass-Evans, R.; Ferrari, M.-C.; Bernardo, P.; Clarizia, G.; Jansen, J. C.; McKeown, N. B. Highly Permeable Benzotriptycene-Based Polymer of Intrinsic Microporosity. *ACS Macro Lett.* **2015**, *4*, 912-915.

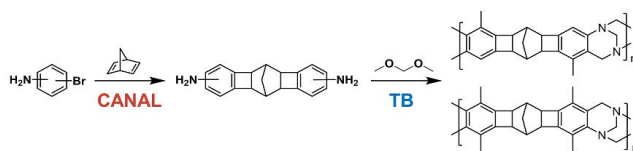
25. Williams, R.; Burt, L. A.; Esposito, E.; Jansen, J. C.; Tocci, E.; Rizzuto, C.; Lanč, M.; Carta, M.; McKeown, N. B. A Highly Rigid and Gas Selective Methanopentacene-based Polymer of Intrinsic Microporosity Derived from Tröger's Base Polymerization. *J. Mater. Chem. A* **2018**, *6*, 5661-5667.
26. Wang, Z.; Wang, D.; Zhang, F.; Jin, J. Tröger's Base-Based Microporous Polyimide Membranes for High-Performance Gas Separation. *ACS Macro Lett.* **2014**, *3*, 597-601.
27. Zhuang, Y.; Seong, J.G.; Do, Y.S.; Jo, H.J.; Cui, Z.; Lee, J.; Lee, Y.M.; Guiver, M.D. Intrinsically Microporous Soluble Polyimides Incorporating Tröger's Base for Membrane Gas Separation, *Macromolecules* **2014**, *47*, 3254-3262.
28. Seong, J.G.; Zhuang, Y.; Kim, S.; Do, Y. S.; Lee, W. H.; Guiver, M. D.; Lee, Y. M. Effect of Methanol Treatment on Gas Sorption and Transport Behavior of Intrinsically Microporous Polyimide Membranes Incorporating Tröger's Base. *J. Membr. Sci.* **2015**, *480*, 104-114.
29. Zhuang, Y.; Seong, J. G.; Do, Y. S.; Lee, W. H.; Lee, M. J.; Guiver, M. D.; Lee, Y. M. High-Strength, Soluble Polyimide Membranes Incorporating Tröger's Base for Gas Separation. *J. Membr. Sci.* **2016**, *504*, 55-65.
30. Lee, M.; Bezzu, C. G.; Carta, M.; Bernardo, P.; Clarizia, G.; Jansen, J. C.; McKeown, N. B. Enhancing the Gas Permeability of Tröger's Base Derived Polyimides of Intrinsic Microporosity. *Macromolecules* **2016**, *49*, 4147-4154.
31. Ghanem, B.; Alaslai, N.; Miao, X.; Pinnau, I. Novel 6FDA-Based Polyimides Derived from Sterically Hindered Tröger's Base Diamines: Synthesis and Gas Permeation Properties. *Polymer* **2016**, *96*, 13-19.
32. Liu, S.; Jin, Z.; Teo, Y. C.; Xia, Y. Efficient Synthesis of Rigid Ladder Polymers via Palladium Catalyzed Annulation. *J. Am. Chem. Soc.* **2014**, *136*, 17434-17437.
33. Lai, H. W. H.; Teo, Y. C.; Xia, Y. Functionalized Rigid Ladder Polymers from Catalytic Arene-Norbornene Annulation Polymerization. *ACS Macro Lett.* **2017**, *6*, 1357-1361.
34. Lai, H. W. H.; Liu, S.; Xia, Y. Norbornyl Benzocyclobutene Ladder Polymers: Conformation and Microporosity. *J. Polym. Sci. A Polym. Chem.* **2017**, *55*, 3075-3081.
35. Teo, Y. C.; Lai, H. W. H.; Xia, Y. Arm-Degradable Star Polymers with Crosslinked Ladder-Motif Cores as a Route to Soluble Microporous Nanoparticles. *Polym. Chem.* **2020**, *11*, 265-269.
36. Lai, H. W. H.; Benedetti, F. M.; Jin, Z.; Teo, Y. C.; Wu, A. X.; Angelis, M. G. D.; Smith, Z. P.; Xia, Y. Tuning the Molecular Weights, Chain Packing, and Gas-Transport Properties of CANAL Ladder Polymers by Short Alkyl Substitutions. *Macromolecules* **2019**, *52*, 6294-6302.
37. Du, N.; Song, J.; Robertson, G. P.; Pinnau, I.; Guiver, M. D. Linear High Molecular Weight Ladder Polymer via Fast Polycondensation of 5,5',6,6'-Tetrahydroxy-3,3',3',3'-tetramethylspirobisindane with 1,4-Dicyanotetrafluorobenzene. *Macromol. Rapid Commun.* **2008**, *29*, 783-788.
38. Song, J.; Du, N.; Dai, Y.; Robertson, G. P.; Guiver, M. D.; Thomas, S.; Pinnau, I. Linear High Molecular Weight Ladder Polymers by Optimized Polycondensation of Tetrahydroxytetramethylspirobisindane and 1,4-Dicyanotetrafluorobenzene. *Macromolecules* **2008**, *41*, 7411-7417.
39. Polak-Kraśna, K.; Dawson, R.; Holyfield, L. T.; Bowen, C. R.; Burrows, A. D.; Mays, T. J. Mechanical Characterisation of Polymer of Intrinsic Microporosity PIM-1 for Hydrogen Storage Applications. *J. Mater. Sci.* **2017**, *52*, 3862-3875.
40. Seaton, N. A.; Walton, J. P. R. B.; Quirke, N. A New Analysis Method for the Determination of the Pore Size Distribution of Porous Carbons from Nitrogen Adsorption Measurements. *Carbon* **1989**, *27*, 853-861.
41. Ma, X.; Pinnau, I. Effect of Film Thickness and Physical Aging on "Intrinsic" Gas Permeation Properties of Microporous Ethanoanthracene-Based Polyimides. *Macromolecules* **2018**, *51*, 1069-1076.

42. Murali, R. S.; Sankarshana, T.; Sridhar, S. Air Separation by Polymer-Based Membrane Technology. *Sep. Purif. Rev.* **2013**, *42*, 130-186.
43. Frisch, H. L. The Time Lag in Diffusion. *J. Phys. Chem.* **1957**, *61*, 93-95.
44. Robeson, L. M. Correlation of Separation Factor versus Permeability for Polymeric Membranes. *J. Membr. Sci.* **1991**, *62*, 165-185.
45. Robeson, L. M. The Upper Bound Revisited. *J. Membr. Sci.* **2008**, *320*, 390-400.

For Table of Contents Use Only

Facile Synthesis and Study of Microporous CANAL-Tröger's Base Ladder Polymers for Membrane Air Separation

Xiaohua Ma, Holden W. H. Lai, Yingge Wang, Abdulrahaman Alhazmi,
Yan Xia,* Ingo Pinnau*



- Facile Synthesis
- High BET Surface Area
- Excellent Mechanical Properties
- High O₂/N₂ Separation Performance

